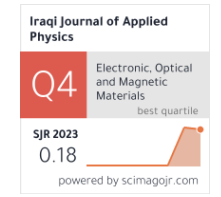
# Samar S. Fazaa Firas A. Najim

Department of Physics, College of Education, University of Al-Qadisiyah, Al-Diwaniyah, IRAQ



# Structural and Electrical Properties of Bi<sub>2</sub>Te<sub>3</sub>:Al Films Prepared by Thermal Evaporation

In order to assess the influence of Al doping on the structural and electrical properties of  $Bi_2Te_3$ , before and after annealing, a range of tests were carried out on samples prepared through thermal evaporation. These tests included x-ray diffraction (XRD) analysis, scanning electron microscopy (SEM), atomic force microscopy (AFM), Hall effect, electrical resistivity, and electrical conductivity. The XRD analysis confirmed the formation of the films, and both SEM and AFM determined that there were no defects in the fabricated films. The addition of Al resulted in a rise in carrier concentration and electrical conductivity, as well as a reduction in electrical resistivity.

**Keywords:** Bi₂Te₃; Doping; Electric properties; Thermal evaporation Received: 18 July 2024; Revised: 07 September; Accepted: 14 September 2024

### 1. Introduction

Thermoelectric materials represent a novel category of functional substances capable of converting thermal energy into electrical energy through the See-beck effect [1]. These materials can be utilized to develop thermoelectric generators or cooling devices, offering benefits such as lightweight construction, small size, long lifespan, environmental friendliness, and suitability for use in harsh environments [2]. It is a heavily doped semiconductor with a narrow energy gap and a rhombohedral crystal structure. The lattice of rhombohedral has been described with a hexagonal layered structure that contains three quintuple layer sequences. The ideal atomic arrangement of the layers is Te(1) - Bi - Te(2)-Bi-Te(1) [3, 4]. The synthesis and optimization of these bismuth chalcogenide thermoelectric materials, especially in low-dimensional form, are crucial for use in the production of micro-scale integrated TE generators and active Peltier cooling devices [5]. There have been several techniques developed for the preparation of Bi<sub>2</sub>Te<sub>3</sub> films, including thermal evaporation[6], sputtering[7], pulse laser deposition (PLD)[8], electrochemical deposition[9], metal organic chemical vapor deposition (MOCVD)[10], and molecular beam epitaxy (MBE) [11]. Although difficult to obtain, MOCVD and MBE deposition techniques are necessary for device applications and microsystem integration that require high-quality epitaxial films with advanced microstructure and composition control. Our paper emphasizes the importance of conventional synthesis methods for developing thermoelectric films with reasonable performance[12], especially for mass production. Elements doped into Bi sites are typically in different valence states, and aluminum can replace the Bi sites in  $Bi_2Te_3$  as it is also in the +3 valence state. This substitution may cause lattice distortion and improve electrical conductivity and thermoelectric properties for Al-doped Bi<sub>2</sub>Te<sub>3</sub>. Furthermore, the use of aluminum can enhance cost efficiency as it is a widely used and inexpensive metal. Therefore, our work aims to study how structural and electrical transport properties can be improved by varying the amounts of doped aluminum in  $Bi_2Te_3$ -based thermoelectric materials (2%, 4%, 6%).

### 2. Experimental Procedures

The preparation of the Bi<sub>2</sub>Te<sub>3</sub> thin films involved thermal evaporation in a high vacuum environment using pure (Bi<sub>2</sub>Te<sub>3</sub>) compound of 99.99% high purity. These films were deposited onto well-cleaned glass substrates, which were cleaned with distilled water and alcohol, then treated in an ultrasonic device for 15 minutes, dried, and prepared for evaporation. A vacuum of (10<sup>-5</sup> m bar) was achieved using a rotary pump and diffusion pump, and the pressure was measured using both the Pirani scale and Penning scale. The films were deposited with a thickness of 100 nm. To create Bi<sub>2</sub>Te<sub>3</sub> films doped with aluminum (Al), the double evaporation (Co-Evaporation) method was employed. In this process, an amount of Bi<sub>2</sub>Te<sub>3</sub> reaching a thickness of 100 nm and aluminum material were placed in molybdenum pots inside the same vacuum chamber, with aluminum added at a weight percentage of 2, 4, or 6% of the Bi<sub>2</sub>Te<sub>3</sub> mass the weight method was used to calculate the thickness. Once the required pressure of  $3.5 \times 10^{-1}$ <sup>5</sup>mbar was reached, deposition was initiated on glass substrates by gradually passing an electric current, allowing the Bi<sub>2</sub>Te<sub>3</sub> and Al to evaporate at different electrode temperatures. Both the pure and doped films were then annealed at (100 °C) for 1 hour, and the structural parameters were subsequently calculated. The lattice constant (a, c) was calculated first due to the hexagonal nature of the films, using Eq. (1) [13]:

$$\frac{1}{d_{hkl}^2} = \frac{4}{3} \left( \frac{h^2 + hk + k^2}{a^2} \right) + \frac{l^2}{c^2} \tag{1}$$

The average crystallite size was calculated by Scherrer's formula) [13]:

$$D_{av} = \frac{k\lambda}{\beta \cos\theta} \tag{2}$$

As for the calculation of the dislocation intensity ( $\delta$ ), we use Eq. (3) [13]:

$$\delta = \frac{1}{D_{av}^2} \tag{3}$$

The number of crystals per unit area  $(N^0)$  was calculated from Eq. (4) [13]:

$$N^0 = \frac{t}{D_{av}^3} \tag{4}$$

The carrier concentration, conductivity and resistivity were calculated using the following equations [13]:

$$R_H = \frac{V_H}{I} \cdot \frac{t}{R} \tag{5}$$

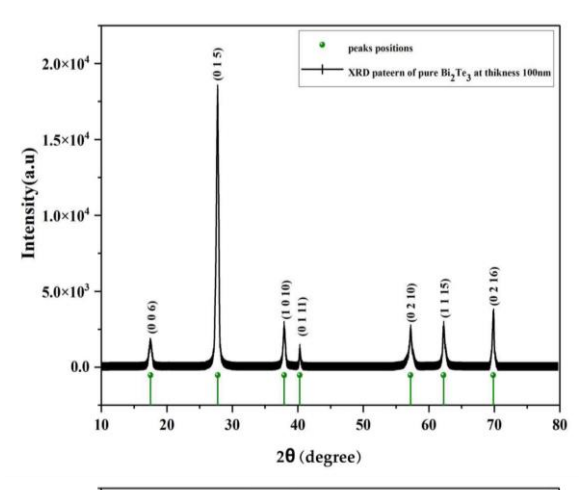
$$\rho = \frac{R \cdot b \cdot t}{L} \tag{6}$$

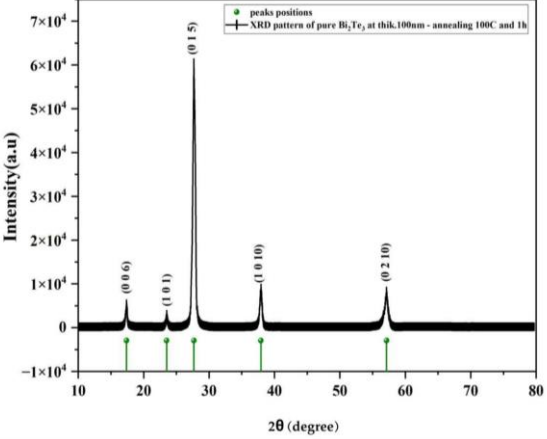
$$\sigma = \frac{1}{2} \tag{7}$$

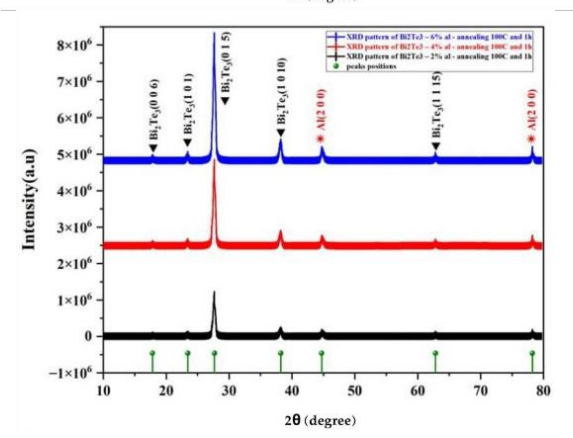
The structure and morphology of the thin film samples were analyzed through X-ray diffraction (XRD, Rigaku D/MAX 2200 PC) with Cu Ka radiation ( $\lambda = 0.154$  nm). Additionally, field emission SEM and EDX were utilized for identification of elements, while atomic force microscopy (AFM) was used for measuring roughness. Film thickness was determined using both a weight-based method and a more precise optical method based on interference in thin films. The samples' hall coefficient, carrier concentration, and mobility were measured using the four-probe method with Vanderbilt Hall measurement system (ECOPIA HMS-3000) at room temperature. Finally, electrical parameters such as continuous electrical conductivity  $(\sigma d. c)$  as a function of temperature and activation energy were also examined.

## 3. Results and Discussion

The XRD patterns of Bi<sub>2</sub>Te<sub>3</sub> pure and doped with Al thin films are displayed in Fig. (1). These films annealed at 100°C for 1 hour. The diffraction peaks were obtained from JCPD data. The pure Bi<sub>2</sub>Te<sub>3</sub> film showed diffraction angles of 17.34°, 27.64°, 37.8°, 41.13°, 56.32°, 62.45° and 69.95° corresponding to (006), (015), (1010), (0111), (0210), (1115) and (0216) diffraction planes. Post-annealing was performed to enhance the thermoelectric properties of these films[14]. The XRD patterns of unannealed and annealed Bi<sub>2</sub>Te<sub>3</sub>/2%Al, Bi<sub>2</sub>Te<sub>3</sub>/4% Al, Bi<sub>2</sub>Te<sub>3</sub>/6% Al films were shown and analyzed. The addition of aluminum resulted in a preferred orientation for the lattice plane (101). The intensity of the aluminum diffraction peak increased with the increase of the doping ratio, but remained weak. The annealing process did not lead to significant changes in the diffraction patterns. However, it did improve the structural integrity of the films. This finding is congruent with references [14]. Our results match those documented under JCPDA CARD No. (89-4302) from American Standard for Testing Materialsas depicted in tables (1) and (2).







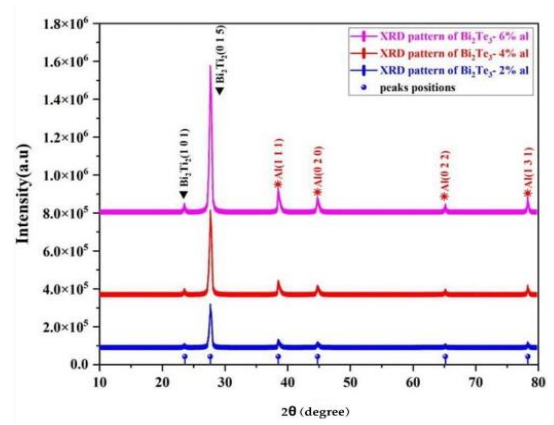


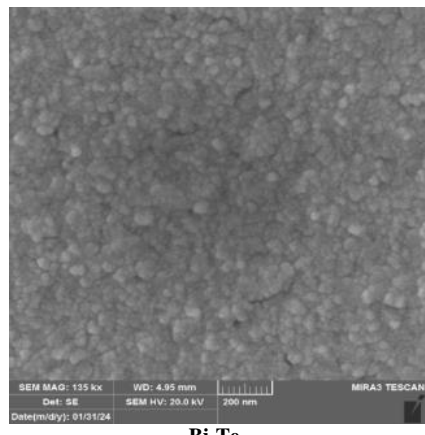
Fig. (1) The XRD patterns for both pure  $Bi_2Te_3$  and  $Bi_2Te_3$  doped with Al. The samples were annealed at  $100^{\circ}C$  and had a film thickness of 100nm

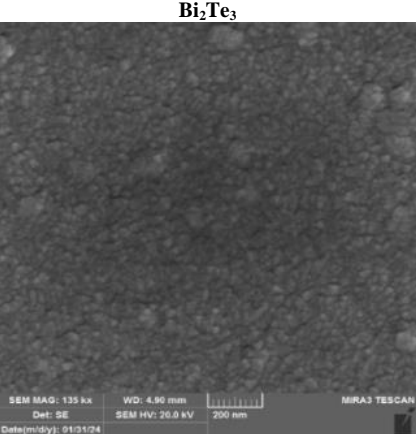
The measurements of the width and height (a, c)of 100 nm thick bismuth telluride (Bi<sub>2</sub>Te<sub>3</sub>) films were determined both prior to and after the annealing process. Eq. (1) from table (3) were used to calculate the measurements of films that had different levels of aluminum doping before and after annealing. It was observed that the doped films had larger lattice constants compared to the standard test card values. Additionally, both pure and doped films displayed similar characteristics before and after annealing. The slight deviation from the original values indicated good crystallization, while larger deviations suggested poor crystallization, which is consistent with previous findings [15]. Furthermore, it was noted that the lattice constants increased when doped with aluminum, confirming that the aluminum atoms occupied positions between the crystals in the structure, as mentioned in ICDD card for Aluminum (96-901-1603) [16].

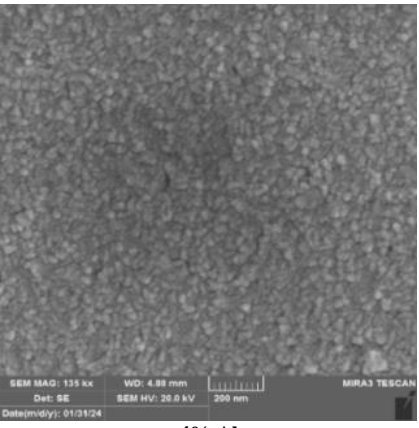
The average size of the crystallite in both pure and doped Bi<sub>2</sub>Te<sub>3</sub> films was determined before and after annealing using Scherer's formula in Eq. (2), focusing on the highest peak in the (015) plane. The results revealed that the average crystallite size increased when the doping ratio rose to 6%, reaching 26.961 nm before annealing and increasing to 25.585 nm after annealing, as shown in table (3). This increase in crystallite size with different doping ratios can be attributed to aluminum atoms occupying interstitial positions in the crystal structure, as well as to grain boundary reorientation due to annealing. It is inferred that the crystallinity of the films improves with annealing temperature, aligning with findings in [17].

Eq. (3) was used to determine the dislocation density of thin films made of pure and aluminum-doped (Bi<sub>2</sub>Te<sub>3</sub>) before and after annealing, based on the crystallite size ratio. Table (3) indicates a gradual increase in dislocation density both before and after annealing. Doping with aluminum led to a decrease in dislocation density, which aligns with the observed decrease in dislocation density with increasing aluminum content, reflecting changes in stress. The trends in dislocation density and lattice stress were found to be similar, with a decrease in dislocation density indicating the production of higher-quality films [18]. As supported by previous research. The alterations in dislocation density also corresponded with modifications in lattice constants.

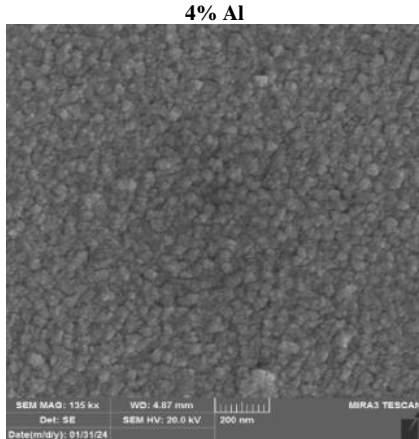
The number of crystals per unit area in 100 nm thick pure  $Bi_2Te_3$  films was determined before and after annealing using Eq. (4). Analysis showed that as the doping ratio increased, the number of crystals per unit area decreased in both the pre- and post-annealing films, as indicated in table (3). This decline in crystal density is attributed to the enlargement of crystallite size, which aligns with the results reported in [19].



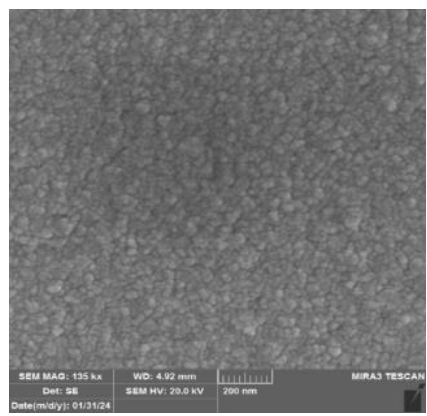




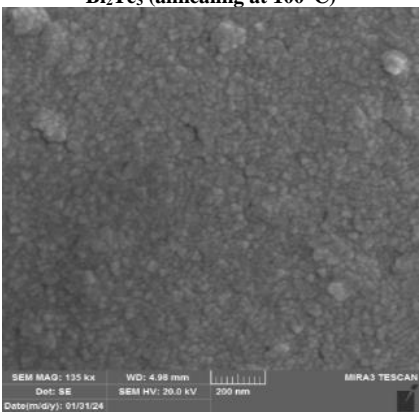
2% Al



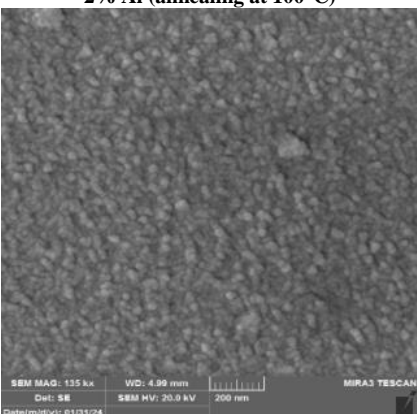
6% Al



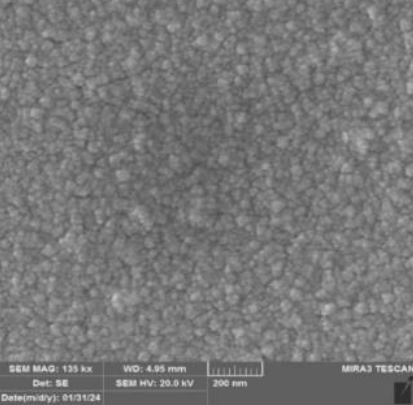
Bi<sub>2</sub>Te<sub>3</sub> (annealing at 100°C)



2% Al (annealing at 100°C)



4% Al (annealing at  $100^{\circ}C)$ 



6% Al (annealing at 100°C)

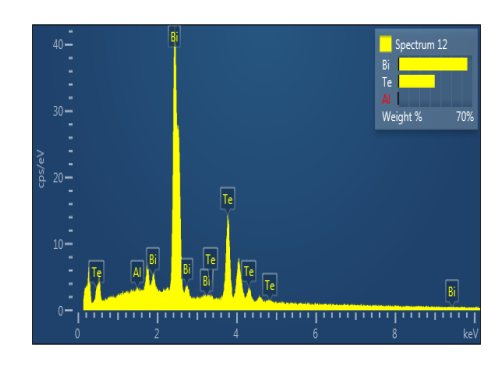


Fig. (2) SEM images showing the morphology of pure  $Bi_2Te_3$  films and those doped with Al, both annealed at  $100^{\circ}C$ . The films are 100 nm thick and were also analyzed using EDX for elemental composition

SEM micrographs show that the samples deposited so far have smooth and consistent surfaces, suggesting that the heat treatment does not dramatically alter the thickness of the film. The surface is composed of tiny crystalline features, some of which seem to clump together in specific areas, indicating that the original samples grow in a mode that results in island-like formations to create the Bi<sub>2</sub>Te<sub>3</sub> compound [20]. The topographic features exhibit minimal changes with heat treatment, implying that the process assists in the diffusion and clumping together of atoms. A comparison of surface images of the original and heat-treated samples in Fig. (2) reveals that improved crystallization occurs after heat treatment, which aligns with the XRD patterns in Fig. (1). The particle size of the heat-treated film is slightly larger than that of the as-deposited film. As the heat treatment temperature increases, the particle boundary becomes less distinct, hinting at a possible reorganization of the surface. This is supported by the fact that the (110) reflection becomes stronger than the (015) reflections in XRD. Furthermore, figure (2) demonstrates that the density of the Al-Bi<sub>2</sub>Te<sub>3</sub> films progressively increases with the aluminum content. The energy-dispersive x-ray spectroscopy (EDX) (Fig. (2) offers a semi-quantitative elemental analysis of the material's surface and verifies the presence of additives in the expected ratio.

Figures (3) and (4) show 3D atomic force microscope (AFM) images of the surfaces of pure and doped Bi<sub>2</sub>Te<sub>3</sub> thin films before and after annealing. The topographic changes and roughness resulting from annealing are evident in these images. Table (4) provides roughness values for the samples. Both pure and doped Bi<sub>2</sub>Te<sub>3</sub> samples exhibit large boulder-like grain islands with smaller features within them. Analysis of XRD data indicates oriented growth along the c-axis, with annealing resulting in smoother island grains. The roughness of the samples ranges from 19 to 54 nm after annealing, with doped films showing a decrease in roughness and non-doped films showing a slight increase. The changes in surface may be due to the suppression of crystal defects, pinholes, and micro-strain relaxation.

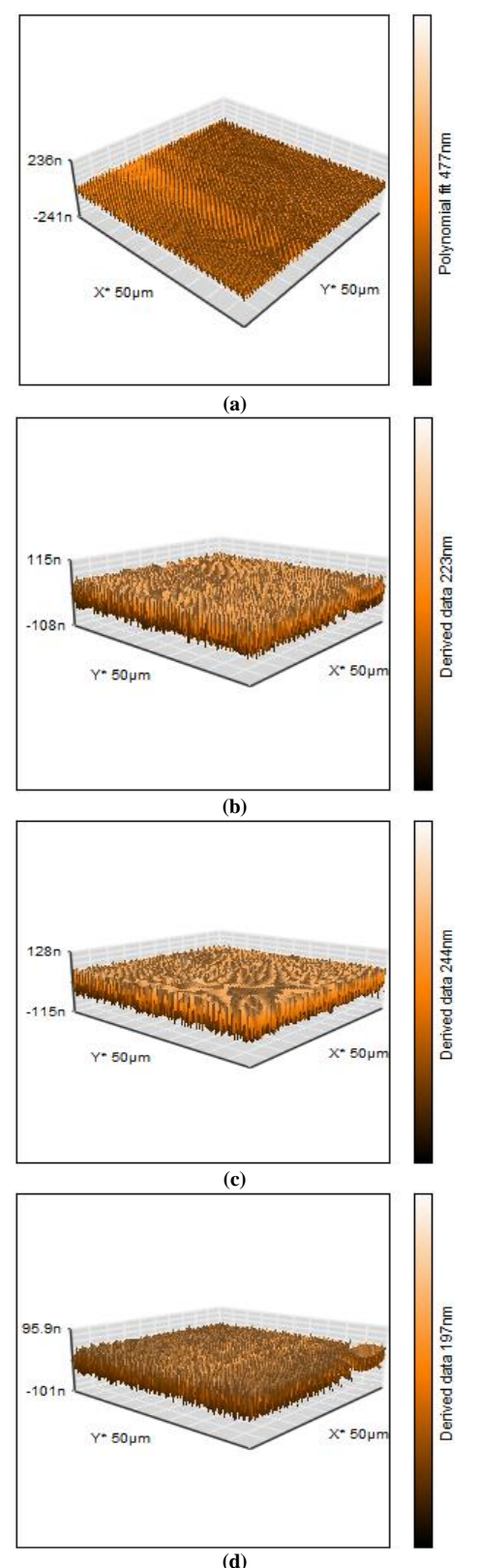


Fig. (1) 3D AFM images for (a)  $Bi_2Te_3$ , (b)  $Bi_2Te_3$ : 2% Al, (c)  $Bi_2Te_3$ : 4% Al, and (d)  $Bi_2Te_3$ : 6% Al, synthesized with thickness of 100nm before annealing

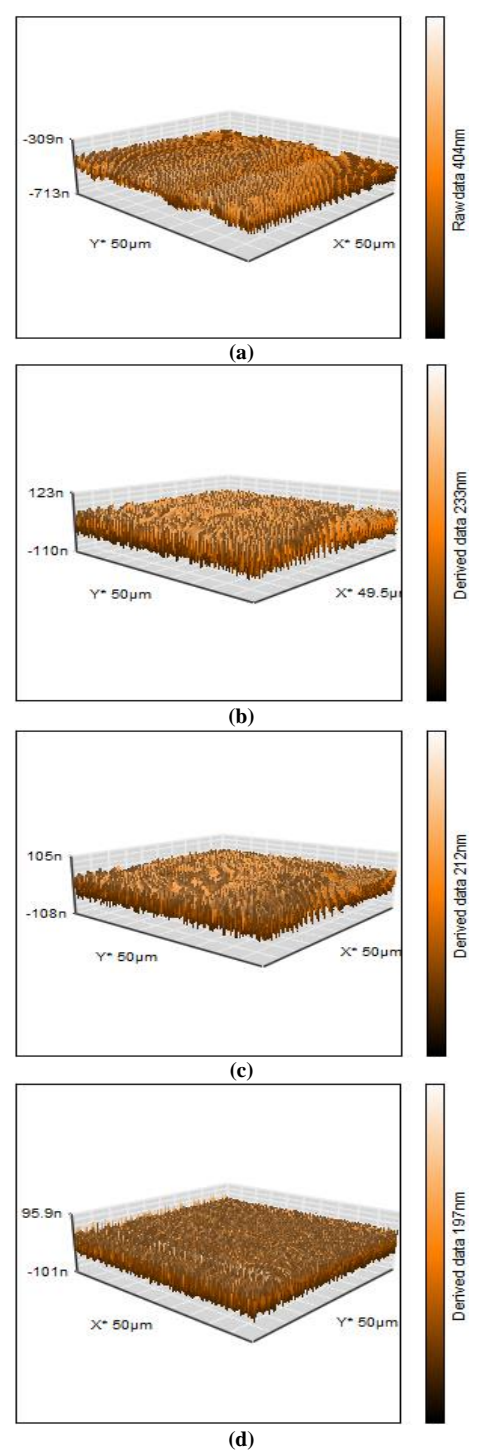
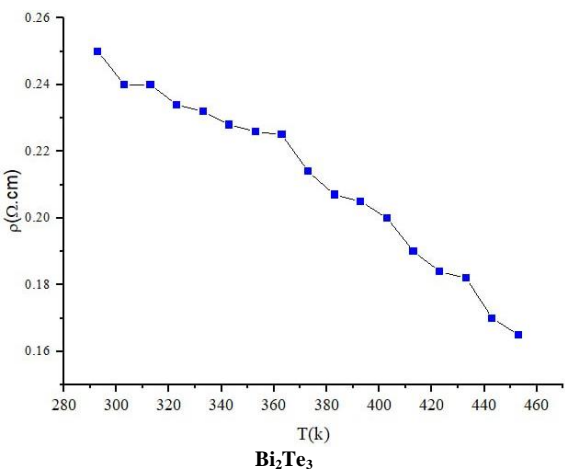


Fig. (2) 3D AFM images for (a)  $Bi_2Te_3$ , (b)  $Bi_2Te_3$ : 2% Al, (c)  $Bi_2Te_3$ : 4% Al, and (d)  $Bi_2Te_3$ : 6% Al, synthesized with thickness of 100nm after annealing

The Hall effect measurements indicate that the concentration and mobility of electron carriers in thin films of pure and 2% Al-doped materials are as follows:  $-3.89\times10^{16}~\rm cm^{-3}$  and  $-2.92\times10^{17}~\rm cm^{-3}$  carriers, and  $2.32\times10^3~\rm cm^2/V.s$  and  $7.42\times10^2~\rm cm^2/V.s$ , as detailed in table (5). The addition of Al significantly increases the electron carrier concentration, but greatly reduces the carrier mobility due to increased lattice defects and grain boundaries in the microstructures in Fig. (3). As a result, the electrical

conductivity of Al-doped Bi<sub>2</sub>Te<sub>3</sub> cannot be improved. At 2% Al doping, the temperature-dependent electrical resistivity displays weak metal-semiconductor transitions, possibly due to enhanced thermal excitations, in line with findings presented by [21].

Fig. (5) illustrates the correlation between temperature and resistivity in a thin film of Bi<sub>2</sub>Te<sub>3</sub>. The resistivity of the Bi<sub>2</sub>Te<sub>3</sub>/2% Al thin film shows minimal variation across various temperatures, but does show a decrease at temperatures lower than 340 K. In comparison, the Bi<sub>2</sub>Te<sub>3</sub> thin film exhibits lower resistivity than the Bi<sub>2</sub>Te<sub>3</sub>/2% Al, consistent with the Hall effect measurement. However, at higher temperatures, the resistivity does not reach zero, indicating an absence of a consistent conducting path. This is linked to the sensitivity of the phase [22].



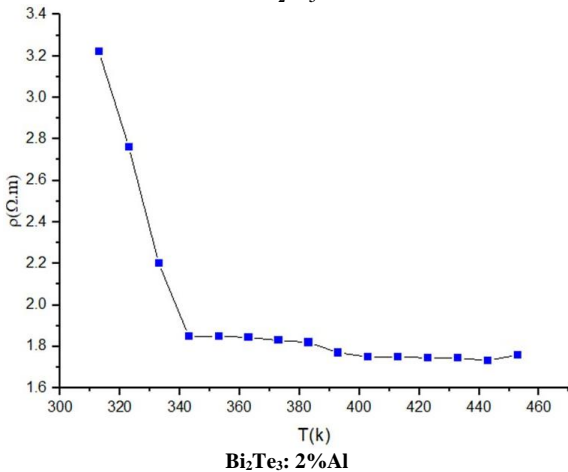


Fig. (5) Electrical resistivity of  $Bi_2Te_3$  films doped with Al (2%) for a thickness of 100nm as a function of temperature

To investigate the impact of temperature and composition on electrical properties, we conducted a study on the electrical conductivity ( $\sigma$ ) of the system at various temperatures, depicted in Fig. (6). Both undoped and doped thin films exhibited a rise in electrical conductivity as the temperature increased. The Bi<sub>2</sub>Te<sub>3</sub>/ 2%Al film displayed a slight uptick in conductivity across the temperature spectrum, with a more notable increase below 340 K. In general, there

was a consistent elevation in electrical conductivity with rising temperature for heavily doped materials, suggesting that a majority of charge carriers are electrons (n-type). This discovery aligns with the findings mentioned in [23].

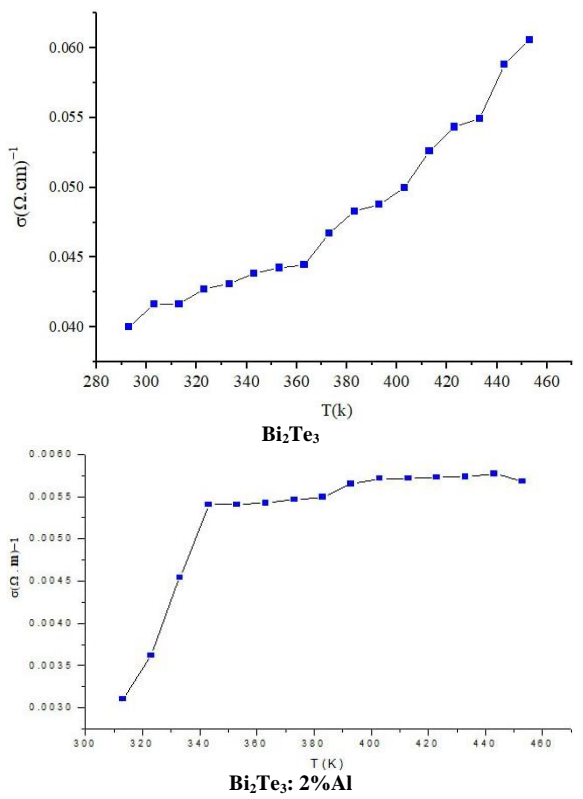


Fig. (6) DC electrical conductivity of Al-doped Bi<sub>2</sub>Te<sub>3</sub> films with thickness of 100nm as a function of temperature

### 4. Conclusions

Through the application of Al dopant and annealing, we have effectively fabricated  $Bi_2Te_3$ -based thin films in our examination. This demonstrates that the inclusion of Al atoms into doped  $Bi_2Te_3$  can augment the electron concentration, leading to an optimal level. The introduction of Al served to reduce electrical resistivity by minimizing scattering and enhancing electrical conductivity. As the structural properties affect the electrical properties in terms of increasing or decreasing charge carriers, in addition to the crystal size affecting the electrical properties.

### References

- [1] T.-R. Wei et al., "Low-Cost and Environmentally Benign Selenides as Promising Thermoelectric Materials", *J. Materiomics*, 4(4) (2018) 304-320.
- [2] N. Salah et al., "Nanocomposites of CuO/SWCNT: Promising Thermoelectric Materials for Mid-Temperature Thermoelectric Generators", J. Euro. Ceram. Soc., 39(11) (2019) 3307-3314.

- [3] J.-W.G. Bos et al., "Structures and Thermoelectric Properties of the Infinitely Adaptive Series (Bi<sub>2</sub>)<sub>m</sub>(Bi<sub>2</sub>Te<sub>3</sub>)<sub>n</sub>", *Phys. Rev. B.*, 75(19) (2007) 195203.
- [4] D.M. Rowe, "Thermoelectrics Handbook: Macro to Nano", CRC Press (2018), p. 1008.
- [5] W. Glatz et al., "Bi<sub>2</sub>Te<sub>3</sub>-Based Flexible Micro Thermoelectric Generator with Optimized Design", *J. Microelectromech. Syst.*, 18(3) (2009) 763-772.
- [6] S. Liu et al., "Study on the Thermoelectric Properties of Porous Bi-Te Films Deposited using Thermal Evaporation on AAO Template", *Curr. Appl. Phys.*, 20(3) (2020) 400-405.
- [7] H. Shang et al., "Synergetic Combination of Te Content and Deposition Temperature to Optimize Thermoelectric Properties using Sputtered Bismuth Telluride Films", *J. Alloys Comp.*, 690 (2017) 851-855.
- [8] H.-C. Chang and C.-H. Chen, "Self-Assembled Bismuth Telluride Films with Well-Aligned Zero-to Three-Dimensional Nanoblocks for Thermoelectric Applications", *Cryst. Eng. Commun.*, 13(19) (2011) 5956-5962.
- [9] Y. Ma et al., "Thermoelectric Characteristics of Electrochemically Deposited Bi<sub>2</sub>Te<sub>3</sub> and Sb<sub>2</sub>Te<sub>3</sub> Thin Films of Relevance to Multilayer Preparation", *J. Electrochem. Soc.*, 159(2) (2011) D50.
- [10] R. Venkatasubramanian et al., "MOCVD of Bi<sub>2</sub>Te<sub>3</sub>, Sb<sub>2</sub>Te<sub>3</sub> and Their Superlattice Structures for Thin-Film Thermoelectric Applications", *J. Cryst. Growth*, 170(1-4) (1997) 817-821.
- [11] Y. Kim et al., "Composition-Dependent Layered Structure and Transport Properties in BiTe Thin Films", *Phys. Rev. B.*, 63(15) (2001) 155306.
- [12] Y. Lei, et al. "High performance thermoelectric materials: progress and their applications", *Adv. Ener. Mater.*, 8(6) (2018) 1701797.
- [13] S.M. Sze, "Semiconductor devices: physics and technology", John-Wiley & Sons (NY, 2008).

- [14] B. Jariwala, D. Shah and N. Ravindra, "Influence of Doping on Structural and Optical Properties of Bi<sub>2</sub>Te<sub>3</sub> Thin Films", *Thin Solid Films*, 589 (2015) 396-402.
- [15] S. Cho et al., "Antisite Defects of Bi<sub>2</sub>Te<sub>3</sub> Thin Films", *Appl. Phys. Lett.*, 75(10) (1999) 1401-1403.
- [16] H.-P. Cheng et al., "Effects of Substrate Temperature on Nanomechanical Properties of Pulsed Laser Deposited Bi<sub>2</sub>Te<sub>3</sub> Films", *Coatings*, 12(6) (2022) 871.
- [17] S. Elahi et al., "Effect of Thickness and Annealing on Structural and Optical Properties of Bi<sub>2</sub>Te<sub>3</sub> Thin Films Prepared from Bi<sub>2</sub>Te<sub>3</sub> Nanoparticels", *Int. J. Thin Film Sci. Technol.*, 3(1) (2014) 13-18.
- [18] R. Sathyamoorthy and J. Dheepa, "Structural Characterization of Thermally Evaporated Bi<sub>2</sub>Te<sub>3</sub> Thin Films", *J. Phys. Chem. Solids*, 68(1) (2007) 111-117.
- [19] R. Sathyamoorthy, S.K. Narayandass, and D. Mangalaraj, "Effect of Substrate Temperature on the Structure and Optical Properties of CdTe Thin Film", Sol. Ener. Mater. Sol. Cells, 76(3) (2003) 339-346.
- [20] J. Zhang et al., "Effect of Annealing Temperature on Microstructure and Thermoelectric Properties of Bismuth–Telluride Multilayer Thin Films Prepared by Magnetron Sputtering", *Mater. Res. Innov.*, 19(sup10) (2015) S10-408-S10-412.
- [21] L. Yao et al., "Effects of Thallium Doping on the Transport Properties of Bi<sub>2</sub>Te<sub>3</sub> Alloy", *J. Electron. Mater.*, 45 (2016) 3053-3058.
- [22] Y.S. Hor et al., "Superconductivity in Cu<sub>x</sub>Bi<sub>2</sub>Se<sub>3</sub> and its Implications for Pairing in the Undoped Topological Insulator", *Phys. Rev. Lett.*, 104(5) (2010) 057001.
- [23] M.-K. Han et al., "Thermoelectric Properties of Bi<sub>2</sub>Te<sub>3</sub>: CuI and the Effect of its Doping with Pb Atoms", *Materials*, 10(11) (2017) 1235.

Table (1) A detailed comparison of the (ASTM) results and the data that was actually observed

Sample	Thickness (nm)	Annealing Temperature	2θ (d) Observed	2θ (d) Standard	d(Å) Standard	d(Å) Observed	FWHM (deg)	Hkl
Bi <sub>2</sub> Te <sub>3</sub>	100	-	27.341	27.634	3.2253	3.25936	0.767	015
	100	100°C	27.398	27.634	3.2253	3.25272	0.98	015

Table (2) Results from X-ray diffraction analysis for pure Bi<sub>2</sub>Te<sub>3</sub> films and Bi<sub>2</sub>Te<sub>3</sub> films doped with aluminum

Sample	Annealing temperature	2θ (degree)	d <sub>hkl</sub> (Å)	FWHM (deg)	Hkl
Bi <sub>2</sub> Te <sub>3</sub> (100 nm)		27.341	3.25936	0.767	015
Bi <sub>2</sub> Te <sub>3</sub> + 2 % Al		27.530	3.24539	1.07	015
Bi <sub>2</sub> Te <sub>3</sub> + 4% Al		27.422	3.25790	0.98	015
Bi <sub>2</sub> Te <sub>3</sub> + 6% Al		27.584	3.23912	0.91	015
Bi <sub>2</sub> Te <sub>3</sub> (100nm)	100 ℃	27.398	3.25272	0.98	015
Bi <sub>2</sub> Te <sub>3</sub> + 2% Al	100 ℃	27.461	3.25336	1.01	015
Bi <sub>2</sub> Te <sub>3</sub> + 4% Al	100 ℃	27.389	3.26178	0.94	015
Bi <sub>2</sub> Te <sub>3</sub> + 6% Al	100 °C	27.528	3.24564	0.89	015

Table (3) Displays the structural parameter findings for purely doped aluminum ( $Bi_2Te_3$ ) films

Material		ckness nm)	Average Crystalline size (nm)	a XRD (Å )	c XRD (Å)	a Standard (Å)	c Standard (Å)	δ×10 <sup>10</sup> (m <sup>-2</sup> )	N° x10¹⁰ (m-²)
Bi <sub>2</sub> Te <sub>3</sub>		100	24.056	4.4534	31.7529	4.3852	30.483	1.728	0.0718
Bi <sub>2</sub> Te <sub>3</sub>	100	100 °C	19.5662	4.4407	31.5094	4.3852	30.483	2.612	0.1335
Bi <sub>2</sub> Te <sub>3</sub> : Al 2%	100		21.335	4.4267	31.2454	4.3852	30.483	2.196	0.103
Bi <sub>2</sub> Te <sub>3</sub> : Al 4%	100		20.491	4.4506	31.699	4.3852	30.483	2.381	0.1162
Bi <sub>2</sub> Te <sub>3</sub> : Al 6%		100	26.961	4.4148	31.0233	4.3852	30.483	1.375	0.051
Bi <sub>2</sub> Te <sub>3</sub> : Al 2%	100	100°C	20.796	4.4419	31.5334	4.3852	30.483	2.312	0.1112
Bi <sub>2</sub> Te <sub>3</sub> : Al 4%	100	100°C	20.617	4.458	31.8427	4.3852	30.483	2.352	0.1141
Bi <sub>2</sub> Te <sub>3</sub> : Al 6%	100	100°C	25.585	4.4272	31.2543	4.3852	30.483	1.527	0.0597

Table (4) Roughness from AFM of as deposited and annealed Bi<sub>2</sub>Te<sub>3</sub> thin films

Sample	Annealing	Root mean square Roughness (nm) Sq	Average Roughness (nm) Sa	
Bi <sub>2</sub> Te <sub>3</sub> (100) nm		28.06	22.44	
Bi <sub>2</sub> Te <sub>3</sub> (100) nm	100°C	30.37	23.99	
Bi <sub>2</sub> Te <sub>3</sub> : 2%Al		29.04	23.05	
Bi <sub>2</sub> Te <sub>3</sub> : 4%Al		36.21	28.36	
Bi <sub>2</sub> Te <sub>3</sub> : 6%Al		20.65	18.42	
Bi <sub>2</sub> Te <sub>3</sub> : 2%Al	100°C	36.06	29.61	
Bi <sub>2</sub> Te <sub>3</sub> : 4%Al	100°C	22.87	19.86	
Bi <sub>2</sub> Te <sub>3</sub> : 6%Al	100°C	31.19	27.95	

 $Table~(5)~Hall~measurements~result~for~pure~Bi_2Te_3~films~doped~with~2\%~aluminum~and~with~a~thickness~of~100nm~and~with~a~t$ 

Sample	Sample Conductivity (Ω. cm)-1		Resistivity (Ω. cm)	Mobility (cm² /V.s)	Carrier concentration (cm <sup>-3</sup> )	
Bi <sub>2</sub> Te <sub>3</sub> (100) nm	1.44E+01	-1.61E+02	3.47E+03	2.32E+03	-3.89E+16	
Bi <sub>2</sub> Te <sub>3</sub> : 2%Al	3.48E+01	-2.14E+01	1.44E+03	7.42E+02	-2.92E+17	